Ventricular Septal Dysfunction Following Surgical Closure of Multiple Ventricular Septal Defects

松久，弘典

(Degree)
博士（医学）
(Date of Degree)
2013-09-11
(Date of Publication)
2014-09-01
(Resource Type)
doctoral thesis
(Report Number)
乙第3229号
(URL)
https://hdl.handle.net/20.500.14094/D2003229

Ventricular Septal Dysfunction Following Surgical Closure of Multiple Ventricular Septal Defects

多発性心室中隔欠損症閉鎖術後の心室中隔機能不全

松久　弘典、芳村　直樹、日隈　智憲、三崎　拓郎、
大沼　芳子、市田　蕗子、大嶋　義博、大北　裕

Key words:　Echocardiography, Myocardial mechanics, Congenital heart disease, Multiple ventricular septal defects, Ventricular septal dysfunction

Abstract

Background. We assessed the global and regional ventricular septal functions using conventional echocardiography and two-dimensional speckle tracking imaging in children with postoperative multiple ventricular septal defects.

Methods. Thirty-six children were studied: 16 children with postoperative multiple ventricular septal defects and 20 normal control subjects. In children with multiple ventricular septal defects, 60 ventricular septal defects were closed using one of three different techniques (patch closure, the sandwich technique, direct closure). Specke tracking imaging was applied to three short-axis echocardiographic images.

Results. The total patch area used in the multiple ventricular septal defects group was correlated with the postoperative ejection fraction (r = 0.703) and Tei index (r = 0.778). The global septal peak systolic radial displacement and global septal peak systolic radial strain in the multiple ventricular septal defects group were significantly lower than those observed in the control subjects. The peak systolic radial strain in the segments closed with patches and the peak systolic radial displacement in the segment closed with the felt sandwich technique were significantly lower than those observed in the intact septal segments. No significant regional functional depressions were identified in the segments that were closed directly.

Conclusions. The postoperative ventricular global and septal functions were significantly reduced in children with multiple ventricular septal defects, especially in the cases with complex congenital heart disease and that were closed with large prosthetic materials. These results suggest that an effort to minimize the use of patch materials may lead to a preserved postoperative ventricular function.

The surgical management of multiple ventricular septal defects (mVSDs) remains controversial and challenging [1-3]. The ideal goal of the treatment for mVSDs is complete obliteration without ventricular dysfunction. A novel technique has been introduced for the closure of muscular ventricular septal defects, which is performed by sandwiching the septum between two felt patches placed in the left and right ventricles (the felt sandwich technique) [4-6]. This technique requires neither ventriculotomy nor transection of muscular trabeculations. Although the felt sandwich technique improves the outcomes of surgical management of patients with mVSDs [4], postoperative cardiac dysfunction caused by the use of numerous felt patches has been reported [5]. Currently, we also use the transatrial re-endocardialization (TAR) technique reported by Alsoufi *et al.* to minimize the number of patches and the incidence of postoperative cardiac dysfunction [7].

Recently, echocardiography-based two-dimensional speckle tracking imaging (2DSTI) has become a validated technique that allows for the quantitative analysis of myocardial wall motion and deformation [8]. We investigated the regional ventricular septal function and its relation to closure techniques using 2DSTI in children who underwent closure of mVSDs.

Patients and Methods

Patient Population

The study design was approved by the institutional review board of the University of Toyama.

Written informed consent was obtained from the parents of all patients. Thirty-six children less than seven years of age were included in this study: 16 children with mVSDs who had undergone biventricular repair and 20 normal controls who were healthy children with structurally and functionally normal echocardiograms were investigated for innocent murmurs or screening purposes. Eight of the 16 patients with mVSDs had associated cardiac anomalies, including double-outlet right ventricle in four cases, tetralogy of Fallot in three cases, and coarctation of the aorta in one case. In the mVSDs group, the median age at operation was 8.0 months (range 3-29 months) and the median weight was 6.6 kg (range 4.9-12.1 kg). Sixty VSDs were closed using three different techniques (patch closure: 17, sandwich technique: 7, direct closure: 36). The location and closure techniques of the mVSDs are shown in Figure 1.

Surgical Strategy and Technique for Muscular VSDs

Our current procedures for muscular VSDs have been previously described [4-6]. Each operation was performed with cardiopulmonary bypass. Following cardioplegic arrest, a longitudinal right atriotomy was made to access the VSDs. The perimembranous VSDs were closed with a Dacron polyester fabric patch. Initially, an attempt was made to close the muscular VSDs with two layers of endocardial running sutures using 6-0 polypropylene sutures [7]. The felt sandwich technique was primarily indicated for large apical or mid-trabecular VSDs [6]. The details of the felt sandwich technique have been described in previous reports. A 3-Fr Nelaton catheter (Bard, Haverhill, Mass), secured to a 4-0 braided polyester suture mounted onto an oversized (2-4 mm larger than the estimated size of the VSD) circular polyester felt patch was grasped by right-angled forceps and pulled back into the right ventricle. The suture ends were then passed through a slightly smaller polyester felt patch. The suture was then tied, thus sandwiching the septum between the two polyester felt patches.

The location and size of the defects and the closure techniques were precisely reported in the operative records according to the classification of Serraf and associates [1].

We hypothesized that the larger area of VSD patches might cause postoperative ventricular septal dysfunction. The total patch area/BSA (body surface area) ratio was calculated based on the following equation: Total VSD patch area/BSA = the sum of all VSD patch area (cm^2)/BSA at repair (m^2), as previously described [5].

Echocardiographic analysis

More than three months after the operation, echocardiography was performed using a Vivid 7 echocardiographic system (GE Medical Systems, Wauwatosa, Wisconsin) with probe frequencies appropriate for the patient size. The left ventricular ejection fraction (LVEF) was determined according to the modified biplane Simpson's method. The left ventricular end-diastolic diameter (LVDd) was also normalized to the patient's body surface area and converted to Z-score based on normal subject measurements [10]. Pulse-wave Doppler was used to measure the ratio between the early and late diastolic transmitral flow velocity (E/A). The Tei index was calculated as the sum of isovolumic contraction time and the isovolumic relaxation time divided by the ejection time, as previously described [11]. For the radial speckle tracking analysis, two-dimensional short axis images of the LV were acquired at the three levels as follows: the basal level (the mitral valve), the midventricular level (the prominent papillary muscles) and the apical level (the LV cavity alone with no visible papillary muscles).

The images were analyzed offline on an Echopac workstation (GE Medical Systems, Wauwatosa, Wisconsin). The endocardial border of each short-axis plane was manually traced. A second larger outer circle was then generated by the computer algorithm, which was manually adjusted to cover the left ventricular myocardium. Then, the software algorithm automatically segmented the LV short-axis plane into six equidistant segments and searched speckles in the region of interest on a frame-by-frame basis using the sum of the absolute difference algorithm. Two (anteroseptum and septum) of the six segments were septal regions (Figure 2). Deformation was assessed according to the peak systolic radial strain (PSRS: percent change in segment thickness during systole, %), peak systolic circumferential strain (PSCS: percent change in segment circumferential length during systole, %) and peak systolic radial displacement (PSRD: myocardial displacement toward the contractile center during systole, mm). To account for changes in heart size, the PSRD was divided by the LVDd (mm) and defined as the percent PSRD (%PSRD, %). The circumferential strain measurements were represented by negative curves. We defined the sum of the PSRS of the six septal segments as the "global septal PSRS," the sum of the PSCS values of the six septal segments as the "global septal PSCS" and the sum of the %PSRD of the six septal segments as the "global septal %PSRD".

In order to assess the influence of the closure technique on the regional ventricular septal function, each septal segment was subdivided into four groups (patch closure, felt sandwich closure, direct closure, intact area) by identifying the patches on echocardiography or referring to the operative records.

Statistical Analysis

Continuous variables were expressed as the mean ± standard deviation. The data were analyzed using the JMP® 9 software program (SAS Institute Inc., Cary, NC, USA). Comparisons of continuous variables between two groups were made using unpaired Student's *t* test or the Wilcoxon rank-sum test as appropriate. Comparisons among more than three groups were made using a one-way analysis of variance (ANOVA) with a post-hoc comparison. The level of statistical significance was set at p = 0.05. Correlations between operative data and echocardiographic parameters were analyzed using a linear regression analysis.

Results

The patient data obtained at examination in the two groups are shown in Table 1. The LVEF was significantly lower in the children with mVSDs than in the normal subjects (69.8 ± 8.3% vs 75.3 ± 4.0 %, p = 0.014). The Z-scores of the LVDd, E/A and Tei-index did not differ between the groups.

Correlation between the Affected Area and the Global Ventricular Function

Figure 3 shows the correlations between the intraoperative data and the echocardiographic parameters of the global ventricular function. The total patch area/BSA was significantly correlated with the postoperative LVEF (r = 0.703, p = 0.0016) and Tei index (r = 0.778, p = 0.0004).

Ventricular Septal Function Assessed on 2DSTI

The myocardial strain and displacement parameters of the ventricular septum are listed in Table 2. The mVSDs group exhibited significantly lower PSCS values than the normal group in the midventricular anteroseptum (p = 0.008) and the midventricular septum (p =0.03). The mVSDs group also exhibited significantly lower global septal PSRS values (p = 0.047). The regional %PSRD values in all regions except the basal septum were significantly lower in the mVSDs group than in the normal group. Therefore, the global septal %RSRD in the mVSDs group was significantly lower than that observed in the normal group (p = 0.0009). In the mVSDs group, the global septal %PSRD was correlated with the postoperative LVEF (r = 0.668, p = 0.0047).

Comparison between Complex and Simple mVSDs

The patients with mVSDs were further subdivided into a complex mVSDs group (with other cardiac anomalies, n = 8) and a simple mVSDs group (without other cardiac anomalies, n = 8). The operative and echocardiographic parameters of the two groups are shown in Table 3. The complex group required longer cardiopulmonary bypass time ($p = 0.04$) and aortic cross-clamp time ($p = 0.02$) than the simple group. The number of VSDs ($p = 0.01$) and the total patch area/BSA ($p = 0.01$) in the complex group were significantly greater than those observed in the simple group. The postoperative LVEF ($p = 0.02$) and the global septal %PSRD ($p = 0.01$) were significantly lower in the complex group. The global septal PSRS ($p = 0.04$) and the global septal %PSRD ($p < 0.001$) in the complex group were significantly lower than those observed in the normal group.

The patients with mVSDs were also subdivided into a right bundle branch block group (n=10) and a normal sinus rhythm group (n=6). There were no significant differences between the groups in terms of patient operative data or postoperative echocardiographic parameters.

Closure Techniques and the Regional Septal Function

Figure 4 summarizes the regional septal speckle tracking parameters of the four groups subdivided by the regional surgical techniques in the children with mVSDs. The PSRS in the segments closed with patches was significantly lower than that observed in the segments without surgical intervention ($p = 0.03$). There was a trend toward a lower PSRS in the segments closed with the felt sandwich technique than in the intact segments ($p = 0.06$). The %PSRD in the segments closed with the felt sandwich technique was significantly lower than that observed in the segments without surgical intervention ($p = 0.02$). There was a trend toward a lower %PSRD in the segments closed with patches than in the intact segments ($p = 0.08$). There were no significant differences in regional PSCS between the four groups.

Comment

Previous surgical reports of mVSDs have focused on postoperative mortality and complications [1, 2]. Reports describing the postoperative ventricular function are limited [3, 6]. Regional measurements of the left ventricular (LV) wall motion on intraoperative transesophageal echocardiography in children with simple VSDs have shown that functional depression after VSD closure is asymmetric, with the greatest decrease localized to the septal and lateral wall segments [11]. In children with mVSDs, assessing the regional ventricular septal function is quite complex but nonetheless important for prognostication and deciding whether the surgical strategy is appropriate.

Although the postoperative LVEF of the mVSDs group was significantly lower than that observed in the control group, its exact value was within the normal range. This may be an effect of our current effort to minimize the amount of patch material used to close VSDs. However, a large total patch area/BSA was strongly correlated with a lower LVEF and a higher Tei index. The Tei index has been reported to be useful for assessing the global LV function and predicting clinical outcomes. Patel and colleague also reported its accuracy and great predictive power in pediatric patients with LV dysfunction, especially those with diastolic and combined dysfunction [12]. Our findings indicate the presence of subclinical LV dysfunction in the mVSDs group. In addition, the total patch area/BSA may be a good predictor of the postoperative global ventricular function.

Recently, 2DSTI that allows for quantitative investigation of regional myocardial wall motion and deformation has been described [8, 13] and its practical application has also been reported in pediatric cases [14-16]. This is the first study to characterize and quantify global and regional wall motion abnormalities in children who underwent closure of mVSDs using 2DSTI. In this study, radial displacement imaging demonstrated that postoperative ventricular septal movement toward the LV contractile center is significantly depressed in children with mVSDs, whereas significant regional depression is detected at the midventricular level according to the peak circumferential strain parameters, and no significant regional depression is observed according to the peak systolic radial strain parameters. This may due to the limited number of cases and variability of 2DSTI parameters in the pediatric population. Marcus and colleagues reported the reference values for 2DSTI in a pediatric and young adult cohort. They found low global peak systolic strain values in infants with a greater range of variation in the youngest age group, particularly at the midventricular level [15]. Although radial displacement images are not widely used to assess the regional ventricular function or as predictors compared with strain images [17], the current study demonstrates that septal movement to the contractile center assumes a vital role in the global ventricular function postoperatively. The use of surgical techniques that preserve radial displacement values leads to a preserved postoperative ventricular function.

We also subdivided the mVSDs group into simple and complex groups. The complex VSDs group had more defects with larger VSD areas, and required longer bypass and cross-clamp time. These factors seem to have affected the postoperative ventricular function in this group. The lower global septal PSRS value observed in the complex mVSDs group indicate depressed viability of the ventricular septum and impaired functional recovery in this group [14]. In addition, we found that the echocardiographic parameters of the postoperative ventricular function in the simple mVSDs group were comparable with those of the normal subjects.

The postoperative regional ventricular septal function of mVSDs may be influenced by several surgical factors, including the use of prosthetic patches in addition to the patch size, suture depth and prolonged cardiac ischemic time [5, 7]. Yoshimura and colleagues reported that 77.8% of patients who underwent the sandwich technique for closure of mVSDs exhibit septal dysfunction on conventional echocardiography [6]. Shin and colleague reported their surgical experience of 20 cases of mVSDs. Although they performed small left ventriculotomy in all cases, they also made efforts to close the VSDs with direct sutures or smaller patches. All of their long-term survivors exhibited a preserved LV function [3]. Our current study quantitatively supports their results using 2DSTI. The sandwich technique may cause regional myocardial ischemia and reduce the contractile reserve. Insertion of solid felt patches itself may inhibit regional contraction [11]. The TAR strategy reported by Alsoufi *et al.* has some theoretical advantages compared to the felt sandwich technique and patch closure [7]. TAR avoids the influence on the left ventricular septal myocardium exerted by patch material. In addition, approximating the right side septal trabeculations using superficial endocardial running sutures may restore the continuity of the viable ventricular septal myocardium and its function. However, it is not easy to place the re-endocardialization sutures in patients with large apical muscular VSDs with poorly defined muscular rims. Such defects are considered suitable for the sandwich technique [6].

Limitations

The primary limitation of this study is its small sample size. In our recent practice, large VSDs tended to be closed using the patch or sandwich technique. In addition to the closure technique, the size of the defect can affect the postoperative ventricular function. The ventricular function is also influenced by the myocardial ischemic time. This study assessed only three levels of the short axis view, and the segmental description of the apical level was not based on the 16 segments recommended by the American Society of Echocardiography or the 17 segments recommended by the American Heart Association. Conducting analysis of the longitudinal strain may add further information regarding the regional ventricular septal function and its association with the global ventricular function. In addition, performing comparisons with other modalities such as cardiac magnetic resonance imaging may help to clarify the regional myocardial viability and predict its functional recovery.

Conclusion

2D speckle tracking imaging allows for the quantitative assessment of the ventricular septal function in children with mVSDs. In this study, the postoperative global ventricular and ventricular septal functions were especially depressed in the patients with complex mVSDs, whereas the parameters observed in the patients with simple mVSDs were comparable to those of normal children. The regional septal functions closed with the patch or sandwich techniques were significantly depressed, and large patch areas were highly correlated with impaired global ventricular functions. These results suggest that an effort to minimize the use of patch material to close VSDs may result in preserved postoperative ventricular functions in this difficult patient group.

References

1. Serraf A, Lacour-Gayet F, Bruniaux J, et al. Surgical management of isolated multiple ventricular septal defects. Logical approach in 130 cases. J Thorac Cardiovasc Surg 1992; 103: 437-42.
2. Kitagawa T, Durham LA 3rd, Mosca RS, Bove EL. Techniques and results in the management of multiple ventricular septal defects. J Thorac Cardiovasc Surg 1998; 115: 848-56.
3. Shin HJ, Jhang WK, Park JJ, et al. Left ventricular function after left ventriculotomy for surgical treatment of multiple muscular ventricular septal defects. Ann Thorac Surg 2011; 92: 1490-3.
4. Ootaki Y, Yamaguchi M, Yoshimura N, Oka S, Yoshida M, Hasegawa T. Surgical management of trabecular ventricular septal defects: the sandwich technique. J Thorac Cardiovasc Surg 2003; 125: 508-12.
5. Murakami H, Yoshimura N, Takahashi H, et al. Closure of multiple ventricular septal defects by the felt sandwich technique: further analysis of 36 patients. J Thorac Cardiovasc Surg 2006; 132: 278-82.
6. Yoshimura N, Matsuhisa H, Otaka S, et al. Surgical management of multiple ventricular septal defects: the role of the felt sandwich technique. J Thorac Cardiovasc Surg 2009; 137: 924-8.
7. Alsoufi B, Karamlou T, Osaki M, et al. Surgical repair of multiple muscular ventricular septal defects: the role of re-endocardialization strategy. J Thorac Cardiovasc Surg 2006; 132: 1072-80.
8. Geyer H, Caracciolo G, Abe H, et al. Assessment of myocardial mechanics using speckle tracking echocardiography: fundamentals and clinical applications J Am Soc Echocardiogr. 2010; 23: 351-69.
9. Kampmann C, Wiethoff CM, Wenzel A, et al. Normal values of M mode echocardiographic measurements of more than 2000 healthy infants and children in central Europe. Heart 2000; 83: 667-72.
10. Eto G, Ishii M, Tei C, Tsutumi T, Akagi T, Kato H. Assessment of global left ventricular function in normal children and in children with dilated cardiomyopathy. J Am Soc Echocardiogr 1999; 12: 1058-64.

11. Quinn TA, Cabreriza SE, Blumenthal BF, et al. Regional functional depression immediately after ventricular septal defect closure. J Am Soc Echocardiogr 2004; 17: 1066-72.
12. Patel DR, Cui W, Gambetta K, Roberson DA. A comparison of Tei index versus systolic to diastolic ratio to detect left ventricular dysfunction in pediatric patients. J Am Soc Echocardiogr 2009; 22: 152-8.
13. Becker M, Lenzen A, Ocklenburg C, et al. Myocardial deformation imaging based on ultrasonic pixel tracking to identify reversible myocardial dysfunction. J Am Coll Cardiol 2008; 51: 1473-81.
14. Friedberg MK, Slorach C. Relation between left ventricular regional radial function and radial wall motion abnormalities using two-dimensional speckle tracking in children with idiopathic dilated cardiomyopathy. Am J Cardiol 2008; 102: 335-9.
15. Marcus KA, Mavinkurve-Groothuis AM, Barends M, et al. Reference values for myocardial two-dimensional strain echocardiography in a healthy pediatric and young adult cohort. J Am Soc Echocardiogr 2011; 24: 625-36.
16. Singh GK, Cupps B, Pasque M, Woodard PK, Holland MR, Ludomirsky A. Accuracy and reproducibility of strain by speckle tracking in pediatric subjects with normal heart and single ventricular physiology: a two-dimensional speckle-tracking echocardiography and magnetic resonance imaging correlative study. J Am Soc Echocardiogr 2010; 23: 1143-52.
17. Cho GY, Marwick TH, Kim HS, Hong KS, Oh DJ. Global 2-dimensional strain as a new prognosticator in patients with heart failure. J Am Coll Cardiol 2009; 54: 618-24.

Table 1. Patient Data Obtained on Examination and Conventional Echocardiographic Parameters

	Control (n=20)	mVSDs (n=16)	*p* Value
Age (months)	26.9 ± 19.7	25.2 ± 12.2	0.76
Height (cm)	81.5 ± 19.2	78.4 ± 12.8	0.57
Weight (kg)	11.1 ± 4.8	9.8 ± 3.1	0.35
Heart rate (bpm)	107 ± 23	114 ± 27	0.35
LVDd (mm)	29.8 ± 5.0	27.9 ± 3.7	0.23
LVDd (Z-score)	1.1 ± 1.5	0.9 ± 1.6	0.69
LVEF (%)	75.3 ± 4.0	69.8 ± 8.3	0.01
E/A	1.62 ± 0.53	1.49 ± 0.15	0.39
Tei index	0.25 ± 0.09	0.33 ± 0.15	0.06

The data are presented as the mean ± standard deviation.

E/A, ratio between the early and late diastolic transmitral flow velocity; VSD, ventricular septal defect; mVSDs, multiple ventricular septal defects; LVDd, left ventricular end-diastolic dimension; LVEF, left ventricular ejection fraction.

Table 2. Speckle Tracking Parameters for Each Septal Segment of the Study Subjects

	Control (n=20)	mVSDs (n=16)	*p* Value
MV-anteroseptum			
PSCS (%)	-21.1 ± 8.5	-19.2 ± 6.8	0.48
PSRS (%)	31.4 ± 15.7	27.5 ± 15.4	0.46
%PSRD (%)	8.69 ± 3.43	5.55 ± 5.38	0.04
MV-septum			
PSCS (%)	-21.0 ± 14.8	-18.7 ± 9.2	0.59
PSRS (%)	30.3 ± 20.8	25.0 ± 18.3	0.43
%PSRD (%)	7.23 ± 4.86	5.37 ± 3.66	0.21
PM-anteroseptum			
PSCS (%)	-23.8 ± 5.9	-18.6 ± 5.0	0.008
PSRS (%)	45.1 ± 17.3	35.8 ± 16.8	0.12
%PSRD (%)	11.53 ± 3.82	6.45 ± 4.86[b]	0.001
PM-septum			
PSCS (%)	-25.0 ± 5.3	-21.3 ± 4.2	0.03
PSRS (%)	49.2 ± 21.0	38.4 ± 20.9	0.13
%PSRD (%)	9.45 ± 3.61	6.11 ± 4.00	0.01
AP-anterosetpum			
PSCS (%)	-22.2 ± 6.4	-20.1 ± 7.8	0.39
PSRS (%)	39.7 ± 21.6	28.2 ± 16.3	0.09
%PSRD (%)	9.00 ± 2.84	6.48 ± 3.56	0.02
AP-septum			
PSCS (%)	-18.7 ± 13.9	-22.8 ± 4.9	0.26
PSRS (%)	45.4 ± 24.2	37.0 ± 17.7	0.25
%PSRD (%)	11.7 ± 4.47	7.00 ± 4.21	0.003
Global septum			
PSCS (%)	-131.8 ± 28.4	-120.8 ± 18.1	0.19
PSRS (%)	241.0 ± 68.5	191.9 ± 74.2	0.047
%PSRD (%)	57.60 ± 15.07	36.97 ± 18.84	0.0009

The data are presented as the mean ± standard deviation.

%PSRD = percent peak systolic radial displacement; AP = apex; MV = mitral valve; PM = papillary muscle; PSCS = peak systolic circumferential strain; PSRS = peak systolic radial strain; VSD = ventricular septal defect.

Table 3. Comparison Between the Complex and Simple mVSDs Groups

	Complex mVSDs (n=8)	Simple mVSDs (n=8)	*p* Value
Operative parameters			
Body weight (kg)	10.5 ± 2.9	9.1 ± 3.3	0.38
BSA (m^2)	0.34 ± 0.05	0.34 ± 0.08	0.91
Cardiopulmonary bypass (min)	201.9 ± 77.3	132.1 ± 21.8	0.04
Cross-clamp time (min)	134.6 ± 49.5	83.8 ± 19.8	0.02
Number of VSDs	4.8 ± 1.9	2.8 ± 0.7	0.01
Total patch area/BSA (cm^2/m^2)	8.16 ± 5.40	2.64 ± 1.48	0.01
Postoperative RBBB	6 (75)	4 (50)	0.60
Echocardiographic parameters			
LVEF (%)	65.3 ± 8.5	74.4 ± 5.2	0.02
E/A	1.44 ± 0.38	1.53 ± 0.39	0.67
Tei index	0.395 ± 0.169	0.265 ± 0.094	0.08
Speckle tracking parameters			
Global septal PSCS (%)	-120.5 ± 15.8	-121.2 ± 21.3	0.95
Global septal PSRS (%)	174.3 ± 87.8	209.5 ± 58.2	0.36
Global septal %PSRD (%)	25.78 ± 10.74	48.15 ± 18.95	0.01

The data are presented as n (percentage) or mean ± standard deviation.

%PSRD = percent peak systolic radial displacement; BSA = body surface area; E/A, ratio between the early and late diastolic transmitral flow velocity; PSCS = peak systolic circumferential strain; PSRS = peak systolic radial strain; RBBB = right bundle branch block; VSD = ventricular septal defect.

Figure Legends

FIGURE 1. Locations of the ventricular septal defects and closure techniques.

FIGURE 2. An example of a patient with multiple ventricular septal defects whose two mid trabecular ventricular septal defects (in the anteroseptum and septum) were individually closed using the sandwich technique. The left ventricular septal wall at the papillary muscle level was automatically subdivided into six segments. The radial displacement curves (left) show impaired systolic myocardial movement toward the contractile center of the anteroseptum (yellow) and septum (red). The radial strain curves (right) show impaired systolic wall thickening of the anteroseptum and septum. (Ant = anterior; AntSept = anteroseptum; Inf = inferior; Lat = lateral; Post = posterior; SAX PM = short axis papillary muscle; Sept = septum)

FIGURE 3. Correlation between the affected total patch area and the postoperative global ventricular function. (BSA = body surface area; VSD = ventricular septal defect)

FIGURE 4. Effects of the surgical techniques on the regional peak systolic radial strain (A) and percent peak systolic radial displacement (B).

Abbreviations and acronyms

2DSTI	= two-dimensional speckle tracking imaging
BSA	= body surface area
E/A	= ratio between the early and late diastolic transmitral flow velocity
LV	= left ventricular
LVDd	= left ventricular end-diastolic diameter
LVEF	= left ventricular ejection fraction
mVSDs	= multiple ventricular septal defects
PSCS	= peak systolic circumferential strain
PSRD	= peak systolic radial displacement
%PSRD	= percent peak systolic radial displacement
PSRS	= peak systolic radial strain
RBBB	= right bundle branch block
TAR	= transatrial re-endocardialization
VSD	= ventricular septal defect

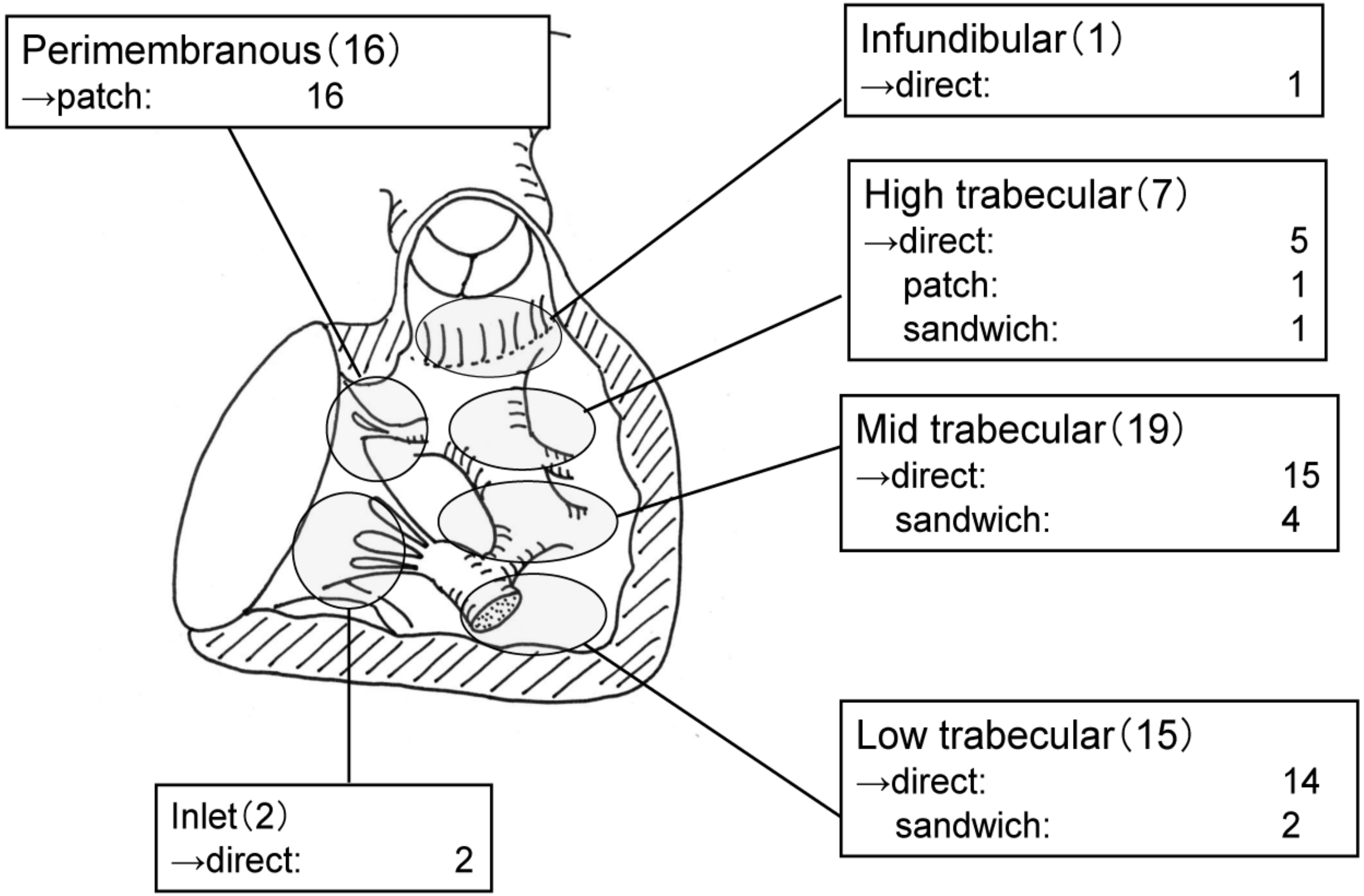
Perimembranous (16)
→patch: 16
Infundibular (1)
→direct: 1
High trabecular (7)
→direct: 5
patch: 1
sandwich: 1
Mid trabecular (19)
→direct: 15
sandwich: 4
Low trabecular (15)
→direct: 14
sandwich: 2
Inlet (2)
→direct: 2

Figure 1

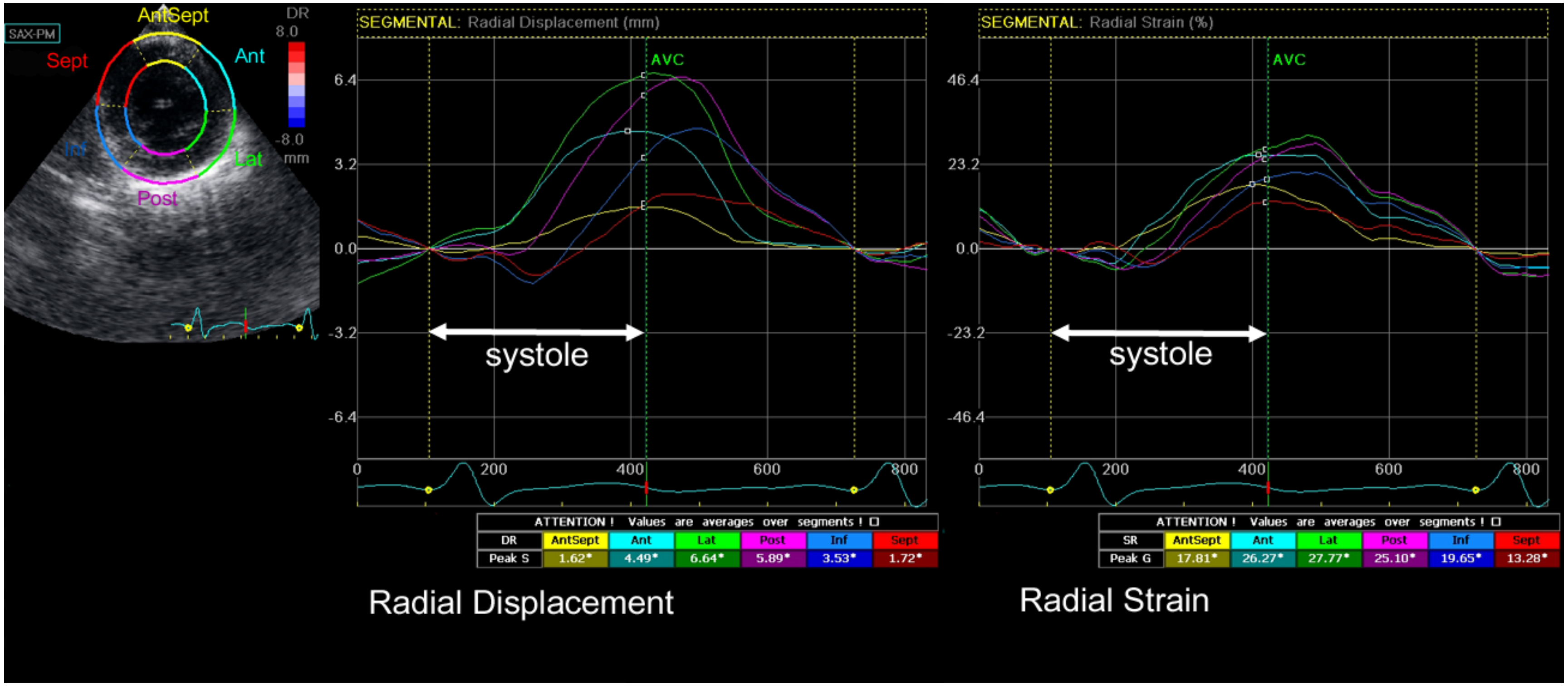
SAX-PM
AntSept
Sept
Ant
Inf
Lat
Post
DR
8.0
-8.0
mm
SEGMENTAL: Radial Displacement (mm)
AVC
6.4
3.2
0.0
-3.2
-6.4
0
200
400
600
800
systole
ATTENTION ! Values are averages over segments !
DR AntSept Ant Lat Post Inf Sept
Peak S 1.62* 4.49* 6.64* 5.89* 3.53* 1.72*
Radial Displacement
SEGMENTAL: Radial Strain (%)
AVC
46.4
23.2
0.0
-23.2
-46.4
0
200
400
600
800
systole
ATTENTION ! Values are averages over segments !
SR AntSept Ant Lat Post Inf Sept
Peak G 17.81* 26.27* 27.77* 25.10* 19.65* 13.28*
Radial Strain

Figure 2

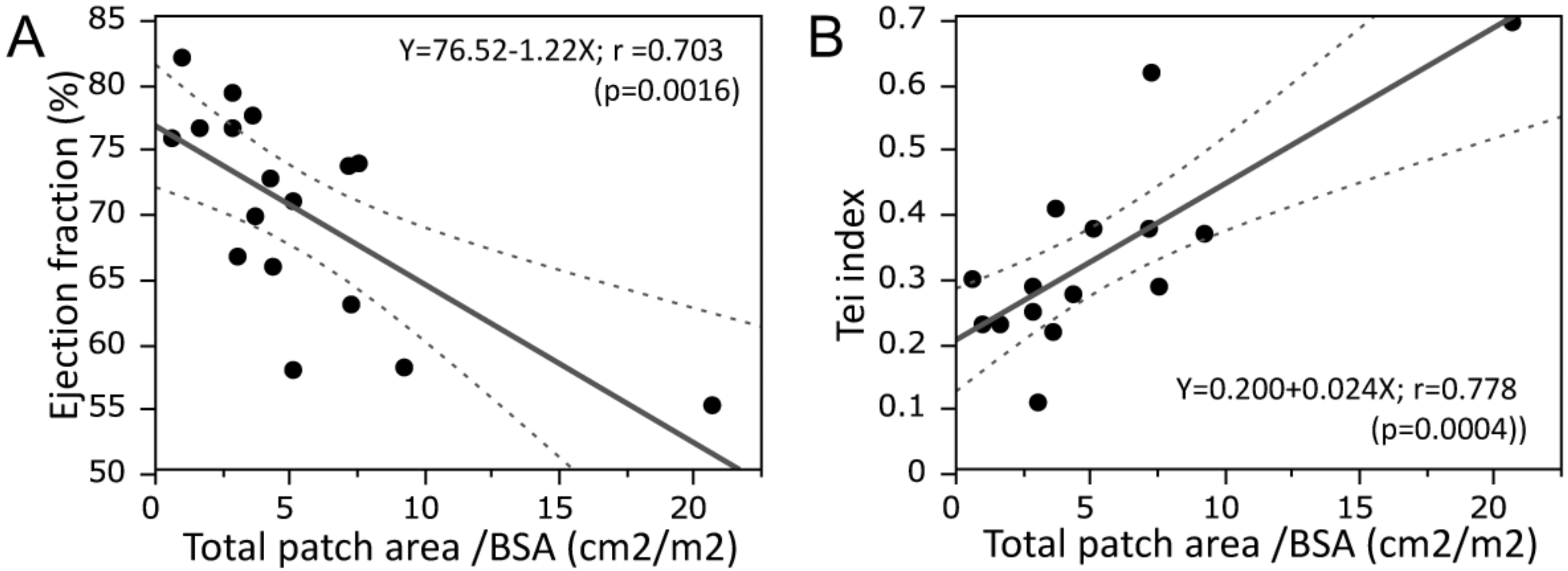
A
Y=76.52-1.22X; r =0.703
(p=0.0016)
Ejection fraction (%)
85
80
75
70
65
60
55
50
0
5
10
15
20
Total patch area /BSA (cm2/m2)
B
Y=0.200+0.024X; r=0.778
(p=0.0004))
Tei index
0.7
0.6
0.5
0.4
0.3
0.2
0.1
0
0
5
10
15
20
Total patch area /BSA (cm2/m2)

Figure 3

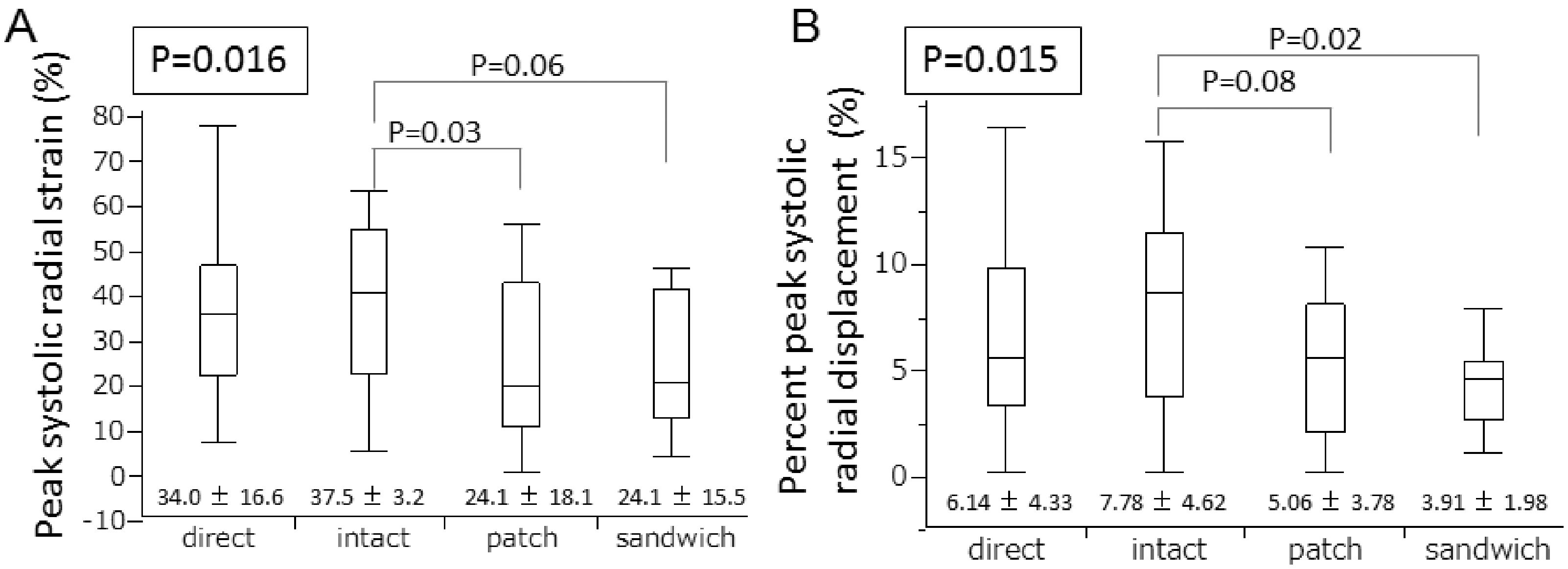

A
P=0.016
P=0.06
P=0.03
Peak systolic radial strain (%)
80
70
60
50
40
30
20
10
0
-10
34.0 ± 16.6
37.5 ± 3.2
24.1 ± 18.1
24.1 ± 15.5
direct
intact
patch
sandwich
B
P=0.015
P=0.02
P=0.08
Percent peak systolic radial displacement (%)
15
10
5
0
6.14 ± 4.33
7.78 ± 4.62
5.06 ± 3.78
3.91 ± 1.98
direct
intact
patch
sandwich

Figure 4